

New physics in semileptonic B decays

B. Capdevila

*Universitat Autònoma de Barcelona,
08193 Bellaterra, Spain*

S. Descotes-Genon*

*Laboratoire de Physique Théorique (UMR 8627), CNRS, Univ. Paris-Sud,
Université Paris-Saclay, 91405 Orsay Cedex, France*

L. Hofer

*Universitat de Barcelona (UB), Martí Franquès 1,
08028 Barcelona, Spain*

J. Matias

*Universitat Autònoma de Barcelona,
08193 Bellaterra, Spain*

J. Virto

*Albert Einstein Center for Fundamental Physics, Institute for Theoretical Physics,
University of Bern, CH-3012 Bern, Switzerland.*

Recently, the LHC has found several anomalies in exclusive semileptonic $b \rightarrow s\ell^+\ell^-$ decays. In this proceeding, we summarise the most important results of our global analysis of the relevant decay modes. After a discussion of the hadronic uncertainties entering the theoretical predictions, we present an interpretation of the data in terms of generic new physics scenarios. To this end, we have performed model-independent fits of the corresponding Wilson coefficients to the data and have found that in certain scenarios the best fit point is preferred over the Standard Model by a global significance of more than 4σ . Based on the results, the discrimination between high-scale new physics and low-energy QCD effects as well as the possibility of lepton-flavour universality violation are discussed.

*Flavor Physics and CP Violation,
6-9 June 2016
Caltech, Pasadena CA, USA*

*Speaker.

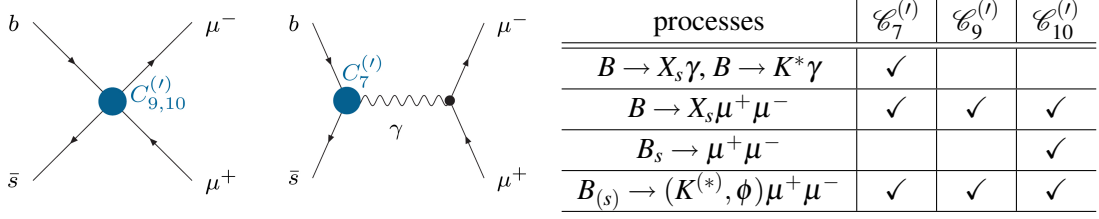


Figure 1: Effective couplings $\mathcal{C}_{7,9,10}^{(l)}$ contributing to $b \rightarrow s \ell^+ \ell^-$ transitions and sensitivity of the various radiative and (semi)leptonic $B_{(s)}$ decays to them.

1. Introduction

The flavour-changing neutral current (FCNC) transition $b \rightarrow s \ell^+ \ell^-$ can be probed through various decay channels, currently studied in detail at the LHC in the LHCb, CMS and ATLAS experiments, as well as at Belle. Recent experimental results have shown interesting deviations from the Standard Model (SM). The LHCb analysis [1] of the 3 fb^{-1} data on $B \rightarrow K^* \mu^+ \mu^-$ in particular confirms a $\sim 3\sigma$ anomaly in two large K^* -recoil bins of the angular observable P'_5 [2, 3] that was already present in the 2013 results with 1 fb^{-1} [4] and subsequently confirmed by the Belle experiment [5]. The observable $R_K = Br(B \rightarrow K \mu^+ \mu^-) / Br(B \rightarrow K e^+ e^-)$ was measured by LHCb [6] in the dilepton mass range from 1 to 6 GeV^2 as $0.745^{+0.090}_{-0.074} \pm 0.036$, corresponding to a 2.6σ tension with its SM value predicted to be equal to 1 (to a very good accuracy). Finally, also the LHCb results [7] on the branching ratio of $B_s \rightarrow \phi \mu^+ \mu^-$ exhibit deviations in two large-recoil bins.

The appearance of several tensions in different $b \rightarrow s \ell^+ \ell^-$ channels is interesting since all these observables are sensitive to the same couplings $\mathcal{C}_{7,9,10}^{(l)}$ induced by the local four-fermion operators in the effective Hamiltonian approach (see Fig. 1)

$$\mathcal{O}_9^{(l)} = \frac{\alpha}{4\pi} [\bar{s} \gamma^\mu P_{L(R)} b] [\bar{\mu} \gamma_\mu \mu], \quad \mathcal{O}_{10}^{(l)} = \frac{\alpha}{4\pi} [\bar{s} \gamma^\mu P_{L(R)} b] [\bar{\mu} \gamma_\mu \gamma_5 \mu], \quad \mathcal{O}_7^{(l)} = \frac{\alpha}{4\pi} m_b [\bar{s} \sigma_{\mu\nu} P_{R(L)} b] F^{\mu\nu},$$

$$\mathcal{C}_9^{\text{SM}}(\mu_b) = 4.07, \quad \mathcal{C}_{10}^{\text{SM}}(\mu_b) = -4.31 \quad \mathcal{C}_7^{\text{SM}}(\mu_b) = -0.29, \quad (1.1)$$

where $P_{L,R} = (1 \mp \gamma_5)/2$, m_b denotes the b quark mass, $\mu_b = 4.8 \text{ GeV}$, and primed operators have vanishing or negligible Wilson coefficients in the SM. It is natural to ask whether a new physics (NP) contribution to these couplings could simultaneously account for the various tensions in the data. Beyond the SM, contributions to $\mathcal{C}_{9,10}^{(l)}$ are for instance generated at tree level in scenarios with Z' bosons or lepto-quarks. Additional scalar or pseudoscalar couplings $\mathcal{C}_{S,S',P,P'}$ cannot address the above-mentioned anomalies since their contributions are suppressed by small lepton masses.

The couplings $\mathcal{C}_{7,9,10}^{(l)}$ can be constrained through various observables in radiative and (semi) leptonic $B_{(s)}$ decays, each of them sensitive to a different subset of coefficients (see Fig. 1). A complete investigation of potential NP effects thus requires a combined study of these observables including correlations. The first analysis in this spirit, performed in Ref. [8] with the data of 2013, pointed to a large negative contribution to the Wilson coefficient \mathcal{C}_9 . This general picture was confirmed later on by other groups, using different/additional observables, different theoretical input for the form factors, etc. (see, e.g., Refs. [9, 10]). We report the most important results of our analysis in Ref. [11] which can be compared to other recent global analyses [12, 13, 14] and

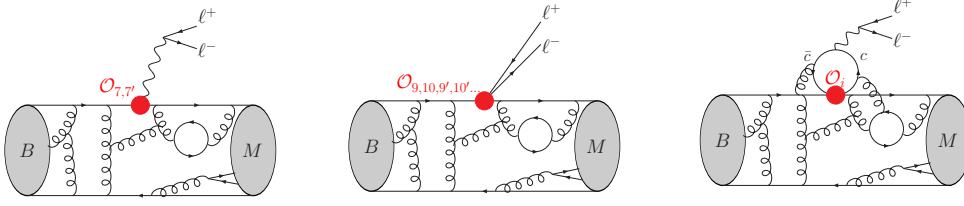


Figure 2: Illustration of factorisable (first two diagrams) and non-factorisable (third diagram) QCD corrections to exclusive $B \rightarrow M \ell^+ \ell^-$ matrix elements.

which improves the original study in Ref. [8] in many aspects: it includes the latest experimental results of all relevant decays (using the LHCb data for the exclusive), it relies on refined techniques to estimate uncertainties originating from power corrections to the hadronic form factors and from non-perturbative charm loops, and consistently takes into account experimental and theoretical correlations. We also discuss the hadronic uncertainties entering the theoretical predictions of the relevant observables and the possibility offered by the presence of NP violating lepton-flavour universality hinted at by R_K .

2. Hadronic uncertainties

Predictions for exclusive semileptonic B decays are plagued by QCD effects of perturbative and non-perturbative nature. At leading order (LO) in the effective theory, predictions involve tree-level diagrams with insertions of the operators $\mathcal{O}_{7,9,10}$ (generated at one loop in the SM), as well as one-loop diagrams with an insertion of the charged-current operator $\mathcal{O}_2 = [\bar{s}\gamma^\mu P_L c][\bar{c}\gamma_\mu P_L b]$ (generated at tree level in the SM). In the first case the leptonic and the hadronic currents factorise, and QCD corrections are constrained to the hadronic $B \rightarrow M$ current (first two diagrams in Fig. 2). This class of *factorisable QCD corrections* thus forms part of the hadronic form factors parametrising the $B \rightarrow M$ transition. Contributions of the second type receive *non-factorisable QCD corrections* (third diagram in Fig. 2) that cannot be absorbed into form factors. In the following we discuss the uncertainties stemming from the two types of corrections and their implementation in our analysis.

2.1 Form factor uncertainties

The form factors are available from lattice QCD as well as from light-cone sum rule (LCSR) calculations, with the former being suited for the region of high $q^2 > 15 \text{ GeV}^2$ and the latter for the region of low $q^2 < 8 \text{ GeV}^2$. Since the form factors introduce a dominant source of theoretical uncertainties, it is desirable to reduce the sensitivity to them as much as possible. For $B \rightarrow V \ell^+ \ell^-$ decays, with V being a vector meson, this can be achieved in the low- q^2 region by exploiting large-recoil symmetries of QCD. At LO in α_s and Λ/m_b , these symmetries enforce certain relations among the seven hadronic form factors $V, A_1, A_2, A_0, T_1, T_2, T_3$, like

$$\frac{m_B(m_B + m_{K^*})A_1 - 2E(m_B - m_{K^*})A_2}{m_B^2 T_2 - 2Em_B T_3} = 1 + \mathcal{O}(\alpha_s, \Lambda/m_b), \quad (2.1)$$

where E denotes the energy of the K^* meson. From the measured coefficients of the differential angular distribution of $B \rightarrow V \ell^+ \ell^-$, we can construct observables that involve ratios like eq. (2.1).

This line of thought, originated in Refs. [15, 16], was later followed by many references (see for instance Refs. [2, 3, 17, 18]). The resulting optimised observables $P_i^{(\prime)}$ only exhibit a mild form factor dependence, suppressed by powers of α_s and Λ/m_b .

For the cancellation of the form factor uncertainties in ratios like the one in eq. (2.1), it is crucial to have control of the correlations among the errors of the different form factors. These correlations can be taken into account via two different approaches: either they can be assessed directly from a LCSR calculation (Ref. [19] provides LCSR form factors with correlation matrices), or they can be implemented resorting to the large-recoil symmetry relations. Whereas the former method is limited to a particular set of form factors (currently only Ref. [19]) and hence sensitive to details of the corresponding calculation, the latter method determines the correlations in a model-independent way from first principles and can thus also be applied to different sets of form factors like the ones from Ref. [20], where no correlations were provided. As a drawback, correlations are obtained from large-recoil symmetries only up to Λ/m_b corrections which have to be estimated. For the estimate of these *factorisable power corrections*, we follow the strategy that was developed in Ref. [21] based on and further refining a method first proposed in Ref. [22]. We assume a generic size of 10% factorisable power corrections to the form factors, which is consistent with the results that are obtained from a fit to the particular LCSR form factors from Refs. [20, 19].

2.2 Uncertainties from $c\bar{c}$ loops

Long-distance charm-loop effects (third diagram in Fig. 2) can mimic the effect of an effective coupling $\mathcal{C}_9^{c\bar{c}}$ and have been suggested as a solution of the anomaly in $B \rightarrow K^* \mu^+ \mu^-$ [23, 24]. Due to the non-local structure of these corrections, their contribution is expected to have a non-constant q^2 -dependence, where q^2 is the squared invariant masses of the lepton pair. Together with the perturbative SM contribution $\mathcal{C}_{9\text{SMpert}}^{\text{eff}}$ and a potential constant NP coupling $\mathcal{C}_9^{\text{NP}}$, it can be cast into an effective Wilson coefficient

$$\mathcal{C}_9^{\text{eff } i}(q^2) = \mathcal{C}_{9\text{SMpert}}^{\text{eff}}(q^2) + \mathcal{C}_9^{\text{NP}} + \mathcal{C}_9^{c\bar{c}i}(q^2), \quad (2.2)$$

with a different $\mathcal{C}_9^{c\bar{c}i}$ and hence also a different $\mathcal{C}_9^{\text{eff } i}$ for the three transversity amplitudes $i = 0, \parallel, \perp$. The evaluation of this long-distance contribution is difficult, especially close to the region of charmonium resonances. Currently, only a partial calculation [20] exists, based on light-cone sum rules combined with a dispersion relation, yielding values $\mathcal{C}_{9\text{KMPW}}^{c\bar{c}i}$ that tend to enhance the anomalies. In our analysis, we assume that this partial result is representative for the order of magnitude of the total charm-loop contribution. When we compute observables in the global fit in the large-recoil region, we assign an error to unknown charm-loop effects varying

$$\mathcal{C}_9^{c\bar{c}i}(q^2) = s_i \mathcal{C}_{9\text{KMPW}}^{c\bar{c}i}(q^2), \quad \text{for } -1 \leq s_i \leq 1. \quad (2.3)$$

3. Results of the global fit

Our reference fits are obtained using the branching ratios and angular observables for $B \rightarrow K^* \mu^+ \mu^-$ and $B_s \rightarrow \phi \mu^+ \mu^-$, the branching ratios of the charged and neutral modes $B \rightarrow K \mu^+ \mu^-$, the branching ratios of $B \rightarrow X_s \mu^+ \mu^-$, $B_s \rightarrow \mu^+ \mu^-$ and $B \rightarrow X_s \gamma$, as well as the isospin asymmetry A_I and the time-dependent CP asymmetry $S_{K^* \gamma}$ of $B \rightarrow K^* \gamma$. For the predictions, we use lattice form

Coefficient	Best fit	1σ	3σ	Pull _{SM}
$\mathcal{C}_7^{\text{NP}}$	-0.02	[-0.04, -0.00]	[-0.07, 0.03]	1.2
$\mathcal{C}_9^{\text{NP}}$	-1.09	[-1.29, -0.87]	[-1.67, -0.39]	4.5
$\mathcal{C}_{10}^{\text{NP}}$	0.56	[0.32, 0.81]	[-0.12, 1.36]	2.5
$\mathcal{C}_7^{\text{NP}}$	0.02	[-0.01, 0.04]	[-0.06, 0.09]	0.6
$\mathcal{C}_9^{\text{NP}}$	0.46	[0.18, 0.74]	[-0.36, 1.31]	1.7
$\mathcal{C}_{10}^{\text{NP}}$	-0.25	[-0.44, -0.06]	[-0.82, 0.31]	1.3
$\mathcal{C}_9^{\text{NP}} = \mathcal{C}_{10}^{\text{NP}}$	-0.22	[-0.40, -0.02]	[-0.74, 0.50]	1.1
$\mathcal{C}_9^{\text{NP}} = -\mathcal{C}_{10}^{\text{NP}}$	-0.68	[-0.85, -0.50]	[-1.22, -0.18]	4.2
$\mathcal{C}_9^{\text{NP}} = -\mathcal{C}_9^{\text{NP}}$	-1.06	[-1.25, -0.85]	[-1.60, -0.40]	4.8

Table 1: Results of one-parameter fits for the Wilson coefficients \mathcal{C}_i considering only $b \rightarrow s\mu\mu$ transitions.

factors from Refs. [25, 26] in the low-recoil region, and LCSR form factors from Ref. [20] (except for $B_s \rightarrow \phi$ where Ref. [19] is used), with correlations assessed from the large-recoil symmetries.

Starting from a model hypothesis with n free parameters for the Wilson coefficients $\{\mathcal{C}_i^{\text{NP}}\}$, we then perform a frequentist fit, including experimental and theoretical correlation matrices. In Tab. 1 we show our results for various one-parameter scenarios. In the last column we give the SM-pull for each scenario, i.e. we quantify by how many sigmas the best fit point is preferred over the SM point $\{\mathcal{C}_i^{\text{NP}}\} = 0$ in the given scenario. A scenario with a large SM-pull thus allows for a big improvement over the SM and a better description of the data. From the results in Tab. 1 we infer that a large negative $\mathcal{C}_9^{\text{NP}}$ is required to explain the data. In a scenario where only this coefficient is generated a fairly good goodness-of-fit is yielded for $\mathcal{C}_9^{\text{NP}} \sim -1.1$. A decomposition into the different exclusive decay channels, as well as into low- and large-recoil regions, shows that each of these individual contributions points to the same solution, i.e. a negative $\mathcal{C}_9^{\text{NP}}$, albeit with different significances. Further results can be found in Ref. [11], e.g., for fits in various 2-parameter scenarios as well as for the full 6-parameter fit of $\mathcal{C}_{7,9,10}^{(\prime)\text{NP}}$ resulting in a SM-pull of 3.6σ .

3.1 New physics vs. non-perturbative charm-contribution

According to Eq. (2.2), a potential NP contribution $\mathcal{C}_9^{\text{NP}}$ enters amplitudes always together with a charm-loop contribution $\mathcal{C}_9^{c\bar{c}i}(q^2)$, spoiling an unambiguous interpretation of the fit result from the previous section in terms of NP. Whereas $\mathcal{C}_9^{\text{NP}}$ does not depend on the squared invariant mass q^2 of the lepton pair, $\mathcal{C}_9^{c\bar{c}i}(q^2)$ is expected to exhibit a non-trivial q^2 -dependence. We show in Fig. 3 on the left a bin-by-bin fit for the one-parameter scenario with a single coefficient $\mathcal{C}_9^{\text{NP}}$. The results obtained in the individual bins are consistent with each other, allowing thus for $\mathcal{C}_9^{\text{NP}}$ constant in the whole q^2 region, as required for an interpretation in terms of NP, though the situation is not conclusive due to the large uncertainties in the single bins.

An alternative strategy to address this question has been followed recently in Ref. [24] where fits of the q^2 -dependent charm contribution $\mathcal{C}_9^{c\bar{c}i}(q^2)$ to the data on $B \rightarrow K^*\mu^+\mu^-$ (at low q^2)

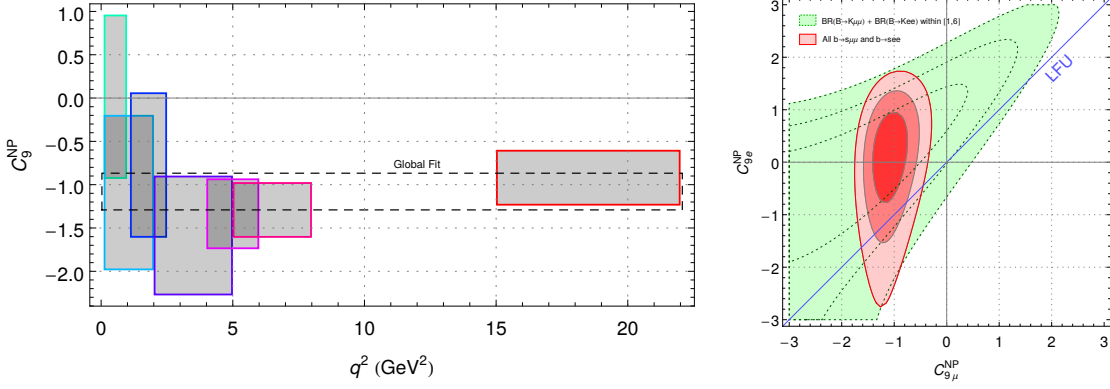


Figure 3: Left: Bin-by-bin fit of the one-parameter scenario with a single coefficient C_9^{NP} for $b \rightarrow s\mu\mu$. Right: Fit with independent coefficients $C_{9\mu}^{\text{NP}}$ and C_{9e}^{NP} , for $b \rightarrow s\mu\mu$ and $b \rightarrow see$ transitions respectively.

has been performed under the hypothesis of the absence of NP. A first fit imposing the results of Ref. [20] for $q^2 \leq 1$ GeV 2 yields a q^2 -dependence suggestive of an unexpectedly large $c\bar{c}$ component. However, this q^2 -dependence comes precisely from imposing specific, purely SM, values at low q^2 and forcing the fit to adopt a skewed and spurious q^2 -dependence. A second fit, without any constraints, yields a result compatible with the results of Ref. [20] supplemented with a constant, helicity-independent, contribution, i.e., C_9^{NP} . The results in Ref. [24] do not allow to draw any conclusions on whether a q^2 -dependent solution of the anomalies via $C_9^{c\bar{c}i}(q^2)$ is preferred compared to a solution via a constant C_9^{NP} since this would require a comparison of the goodness of the fit taking into account the different number of free parameters of the two parametrizations (or other equivalent tools, such as the information criterion of these two hypotheses, not considered in Ref. [24]). Moreover, we should stress that the results for the observables presented in Ref. [24] should not be interpreted as SM predictions, as they are based on a fit to the experimental data.

3.2 Lepton-flavour universality violation

Since the measurement of R_K suggests the violation of lepton-flavour universality, we also studied the situation where the muon- and the electron-components of the operators $\mathcal{O}_{9,10}^{(n)}$ receive independent NP contributions $C_{9\mu}^{\text{NP}}$ and C_{9e}^{NP} , respectively. The electron-couplings C_{9e}^{NP} are constrained by adding $B \rightarrow K^{(*)}e^+e^-$ to the global fit [6, 27]. The correlated fit to $B \rightarrow K\mu^+\mu^-$ and $B \rightarrow Ke^+e^-$ simultaneously is equivalent to a direct inclusion of the observable R_K . In Fig. 3 on the right we display the result for the two-parameter fit to the coefficients $C_{9\mu}^{\text{NP}}$ and C_{9e}^{NP} . The fit prefers a scenario with NP coupling to $\mu^+\mu^-$ but not to e^+e^- . Under this hypothesis, that should be tested by measuring R_{K^*} and R_ϕ , the SM-pull increases by $\sim 0.5\sigma$ compared to the value in Tab. 1 for the lepton-flavour universal scenario.

We expect in a near future to have experimental analyses for electron as well as muon for the various decay modes. In Ref. [28], we have discussed how angular analyses of $B \rightarrow K^*ee$ and $B \rightarrow K^*\mu\mu$ decay modes can be combined to understand better the pattern of anomalies observed and to get a solid handle on the size of some SM long-distance contributions. We can introduce the following observables: $Q_i = P_i^\mu - P_i^e$ and $B_i = J_i^\mu / J_i^e - 1$ associated with the optimised observables

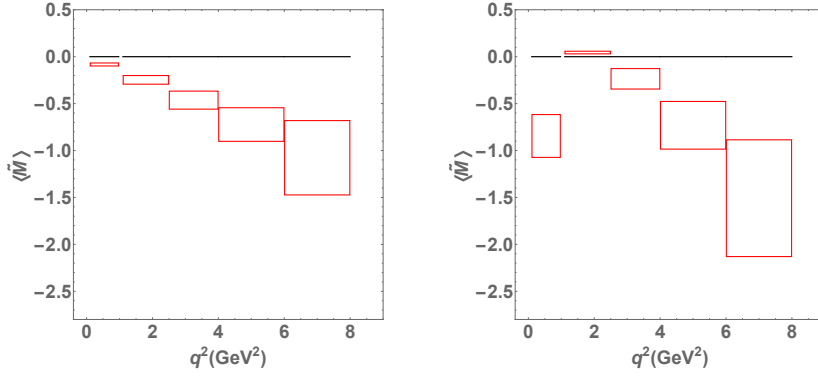


Figure 4: Predictions (in red) for the observable \tilde{M} in two different NP scenarios violating lepton-flavour universality: $\mathcal{C}_{9\mu}^{\text{NP}} = -1.1, \mathcal{C}_{ie}^{\text{NP}} = 0$ (left), $\mathcal{C}_{9\mu}^{\text{NP}} = \mathcal{C}_{10\mu}^{\text{NP}} = -0.65, \mathcal{C}_{ie}^{\text{NP}} = 0$ (right).

P_i and the angular coefficients J_i describing the geometry of the $B \rightarrow K^* \ell \ell$ decay. A measurement of Q_i different from zero would point to NP in an unambiguous way, confirming the violation of lepton flavour universality observed in R_K . In addition B_5 and B_{6s} exhibit only a linear dependence on $C_{9\ell}$ at large recoil providing further possibilities to disentangle the contributions coming from NP in C_9 and C_{10} , with a clean separation between lepton-flavour dependent (NP) and lepton-flavour universal (NP or SM long-distance) contributions to C_9 . We can also build the observable \tilde{M}

$$\tilde{M} = (\beta_e^2 J_5^\mu - \beta_\mu^2 J_5^e)(\beta_e^2 J_{6s}^\mu - \beta_\mu^2 J_{6s}^e) / [\beta_e^2 \beta_\mu^2 (J_{6s}^\mu J_5^e - J_{6s}^e J_5^\mu)]. \quad (3.1)$$

which exhibits very interesting features: in the presence of lepton-flavour non-universal NP in $C_{9\ell}$ or $C_{10\ell}$ only, the large-recoil expression for \tilde{M} is independent of long-distance lepton-flavour universal contributions (in particular transversity-independent charm contributions) and provides clean signals of NP. In Ref. [28], several NP scenarios compatible with the global fit in Ref. [11] are disentangled with the help of these clean observables measuring lepton-flavour non-universality.

4. Conclusions

LHCb data on $b \rightarrow s \ell^+ \ell^-$ decays shows several tensions with SM predictions, in particular in the angular observable P_5' of $B \rightarrow K^* \mu^+ \mu^-$, in the branching ratio of $B_s \rightarrow \phi \mu^+ \mu^-$, and in the ratio R_K (all of them at the $\sim 3\sigma$ level). In global fits of the Wilson coefficients to the data, scenarios with a large negative $\mathcal{C}_9^{\text{NP}}$ are preferred over the SM by typically more than 4σ . A bin-by-bin analysis demonstrates that the fit is compatible with a q^2 -independent effect generated by high-scale new physics, though a q^2 -dependent QCD effect cannot be excluded with the current precision. Note, however, that a QCD effect could not explain the tension in R_K . The latter observable further favours a lepton-flavour non-universal scenario with NP coupling only to $\mu^+ \mu^-$ but not to $e^+ e^-$, a scenario to be probed by a measurement of analogous ratios for other observables.

Acknowledgments

SDG, JM and JV acknowledge financial support from FPA2014-61478-EXP. The work of L.H. was supported by the grants FPA2013-46570-C2-1-P and 2014-SGR-104, and partially by the

Spanish MINECO under the project MDM-2014-0369 of ICCUB (Unidad de Excelencia “María de Maeztu”). JV is funded by the DFG within research unit FOR 1873 (QFET), and acknowledges financial support from CNRS. This project has received funding from the EU Horizon 2020 research and innovation programme under grant agreements No 690575, No 674896 and No. 692194.

References

- [1] R. Aaij *et al.* [LHCb Collaboration], JHEP **1602** (2016) 104 [arXiv:1512.04442 [hep-ex]].
- [2] S. Descotes-Genon *et al.*, JHEP **1301** (2013) 048, arXiv:1207.2753 [hep-ph].
- [3] S. Descotes-Genon *et al.*, JHEP **1305** (2013) 137, arXiv:1303.5794 [hep-ph].
- [4] LHCb Collaboration, PRL **111** (2013) 191801, arXiv:1308.1707 [hep-ex].
- [5] A. Abdesselam *et al.* [Belle Collaboration], arXiv:1604.04042 [hep-ex].
- [6] LHCb Collaboration, Phys. Rev. Lett. **113** (2014) 151601, arXiv:1406.6482 [hep-ex].
- [7] LHCb Collaboration, JHEP **1307** (2013) 084, arXiv:1305.2168 [hep-ex].
- [8] S. Descotes-Genon, J. Matias and J. Virto, Phys. Rev. D **88** (2013) 074002, arXiv:1307.5683 [hep-ph].
- [9] W. Altmannshofer and D. M. Straub, Eur. Phys. J. C **73** (2013) 2646 arXiv:1308.1501 [hep-ph].
- [10] F. Beaujean, C. Bobeth and D. van Dyk, Eur. Phys. J. C **74** (2014) 2897 [Eur. Phys. J. C **74** (2014) 3179], arXiv:1310.2478 [hep-ph].
- [11] S. Descotes-Genon *et al.*, JHEP **1606** (2016) 092, arXiv:1510.04239 [hep-ph].
- [12] W. Altmannshofer and D. M. Straub, Eur. Phys. J. C **75** (2015) 8, 382, arXiv:1411.3161 [hep-ph].
- [13] W. Altmannshofer and D. M. Straub, arXiv:1503.06199 [hep-ph].
- [14] T. Hurth, F. Mahmoudi and S. Neshatpour, Nucl. Phys. B **909** (2016) 737, arXiv:1603.00865 [hep-ph].
- [15] F. Kruger and J. Matias, Phys. Rev. D **71** (2005) 094009, hep-ph/0502060.
- [16] B. Grinstein and D. Pirjol, Phys. Rev. D **70** (2004) 114005, hep-ph/0404250.
- [17] J. Matias *et al.* JHEP **1204** (2012) 104, arXiv:1202.4266 [hep-ph].
- [18] C. Bobeth, G. Hiller and D. van Dyk, JHEP **1007** (2010) 098, arXiv:1006.5013 [hep-ph].
- [19] A. Bharucha, D. M. Straub and R. Zwicky, arXiv:1503.05534 [hep-ph].
- [20] A. Khodjamirian *et al.*, JHEP **1009** (2010) 089, arXiv:1006.4945 [hep-ph].
- [21] S. Descotes-Genon *et al.*, JHEP **1412** (2014) 125, arXiv:1407.8526 [hep-ph].
- [22] S. Jäger and J. Martin Camalich, JHEP **1305** (2013) 043, arXiv:1212.2263 [hep-ph].
- [23] J. Lyon and R. Zwicky, arXiv:1406.0566 [hep-ph].
- [24] M. Ciuchini *et al.*, JHEP **1606** (2016) 116, arXiv:1512.07157 [hep-ph].
- [25] R. R. Horgan, Z. Liu, S. Meinel and M. Wingate, Phys. Rev. D **89** (2014) 9, 094501, arXiv:1310.3722 [hep-lat], PoS LATTICE **2014** (2015) 372, arXiv:1501.00367 [hep-lat].
- [26] C. Bouchard *et al.* [HPQCD Collaboration], Phys. Rev. D **88** (2013) 5, 054509 [Phys. Rev. D **88** (2013) 7, 079901], arXiv:1306.2384 [hep-lat].
- [27] R. Aaij *et al.* [LHCb Collaboration], JHEP **1504** (2015) 064, arXiv:1501.03038 [hep-ex].
- [28] B. Capdevila *et al.*, arXiv:1605.03156 [hep-ph].